Time-Resolved Resonance Raman Elucidation of the Pathway for Dioxygen Reduction by Cytochrome *c* Oxidase

Takashi Ogura,† Satoshi Takahashi,† Shun Hirota,† Kyoko Shinzawa-Itoh,‡ Shinya Yoshikawa,‡ Evan H. Appelman,§ and Teizo Kitagawa*,†

Contribution from the Institute for Molecular Science, Okazaki National Research Institutes/ Department of Functional Molecular Science, Graduate University for Advanced Studies, Myodaiji, Okazaki, 444 Japan, Department of Life Science, Faculty of Science, Himeji Institute of Technology, 1479-1 Kanaji, Kamigoricho, Akogun, Hyogo 678-12, and Chemistry Division, Argonne National Laboratory, Argonne, Illinois 60439

Received February 3, 1993

Abstract: Time-resolved resonance Raman (RR) spectra were observed for catalytic intermediates of bovine cytochrome *c* oxidase at room temperature by using an Artificial Cardiovascular System for Enzymatic Reactions and Raman/ Absorption Simultaneous Measurement Device. The isotope-frequency-shift data using an asymmetrically labeled dioxygen, $^{16}O^{18}O$, established that the primary intermediate (compound **A**) is an end-on-type dioxygen adduct of cytochrome a_3. Higher resolution RR experiments revealed that the ~800-cm^{-1} band assigned previously to the Fe^{IV}=O stretching mode of the subsequent intermediate (compound **B**) was actually composed of two bands that behaved differently upon deuteration. The 804/764-cm^{-1} pair for the $^{16}O_2/^{18}O_2$ derivatives were insensitive to deuteration, and these bands became noticeably stronger at higher temperatures. In contrast, the 785/751-cm^{-1} pair for the $^{16}O_2/^{18}O_2$ derivatives was shifted to 796/766 cm^{-1} in D_2O, and its intensity became virtually zero at 30 °C. The corresponding bands for the $^{16}O^{18}O$ derivative appeared at nearly the same frequencies as those of the $^{16}O_2$ and $^{18}O_2$ derivatives but not at an intermediate frequency. Therefore, neither of these bands could be attributed to the O–O stretching mode. Normal coordinate calculations using a set of suitable force constants of the Urey–Bradley–Shimanouchi force field for an isolated Fe–O–O–H group could explain the 785/751-cm^{-1} bands in terms of the Fe–O stretching vibration, although this model assumed a relatively strengthened Fe–O bond and weakened O–O bond for the Fe–O–O–H group. The 804/764-cm^{-1} bands were assigned to the Fe^{IV}=O stretching mode of the ferryl intermediate. The 356/342-cm^{-1} pair for the $^{16}O_2/^{18}O_2$ derivatives was insensitive to deuteration, and its frequencies were the same as those obtained with $^{16}O^{18}O$. The intensities of the components of this pair were appreciable even when those of the 785/751-cm^{-1} pair were zero. Therefore, contrary to the previous assignment, the 356/342-cm^{-1} pair cannot be ascribed to the hydroperoxy intermediate, but its intensity behavior with temperature was also not coincident with that of the 804/764-cm^{-1} pair. Although the assignment of the 356/342-cm^{-1} pair is yet to be determined, the present experiments have conclusively established that the main pathway for dioxygen reduction by cytochrome *c* oxidase is Fe^{II}—O_2 → Fe^{III}—O—O—H → Fe^{IV}=O → Fe^{III}—OH and that their key bands for the $^{16}O_2/^{18}O_2$ pair are at 571/544, 785/751, 804/764, and 450/425 cm^{-1}, respectively.

Cytochrome *c* oxidase (CcO) [EC 1.9.3.1.] is the terminal enzyme of the respiratory chain of aerobic organisms.[1,2] This enzyme couples the electron transfer from cytochrome *c* to molecular oxygen with the vectorial proton translocation across the membrane. Mitochondrial CcO has two heme A groups and two copper ions as redox-active metal centers per functional unit with 13 polypeptides, the molecular weight being 200 kD.[3] CcO can be functionally divided into two parts, cytochrome *a* and cytochrome a_3. Cytochrome *a* has a six-coordinate low-spin heme A (Fe_a) and an EPR-visible copper (Cu_A), mediating electrons from cytochrome *c* to cytochrome a_3. Cytochrome a_3 also contains heme A (Fe_{a3}), which is five-coordinate high-spin in the reduced state, and an EPR-invisible copper (Cu_B). It was suggested that Fe_{a3}^{III} ($S = {}^5/_2$) and Cu_B^{II} ($S = {}^1/_2$) were antiferromagnetically coupled, probably via a sulfur ligand in the resting state.[4]

The reaction of CcO has been extensively studied by time-resolved absorption,[5–8] cryogenic absorption,[9–12] and EPR spectroscopy.[13–15] Resonance Raman (RR) spectroscopy has been acknowledged to be a powerful technique for studying the structure of the catalytic site of heme proteins and has provided both kinetic and structural information for the enzyme in solution.[16,17] In fact, RR spectroscopy has been applied to reaction intermediates of peroxidases[18,19] and cytochrome P-450.[20–22] More recently, time-resolved resonance Raman (TR^3) spectroscopy has yielded

* Author to whom correspondence should be addressed.
† Graduate University for Advanced Studies.
‡ Himeji Institute of Technology.
§ Argonne National Laboratory.

(1) Babcock, G. T.; Wikström, M. *Nature* **1992**, 356.
(2) Chan, S. I.; Li, P. M. *Biochemistry* **1990**, *29*, 1–12.
(3) Buse, G.; Meinecke, L.; Bruch, B. *J. Inorg. Biochem.* **1985**, *23*, 149–153.
(4) Powers, L.; Chance, B.; Ching, Y.; Angiolillo, P. *Biophys. J.* **1981**, *34*, 465–498.
(5) Gibson, Q.; Greenwood, C. *Biochem. J.* **1963**, *86*, 541–554.
(6) Hill, B. C.; Greenwood, C. *Biochem. J.* **1984**, *218*, 913–921.
(7) Orii, Y. *Ann. N. Y. Acad. Sci.* **1988**, *550*, 105–117.
(8) Oliveberg, M.; Brzezinski, P.; Malmström, B. G. *Biochim. Biophys. Acta* **1989**, *977*, 322–328.
(9) Chance, B.; Saronio, C.; Leigh, J. S., Jr., *J. Biol. Chem.* **1975**, *250*, 9226–9237.
(10) Chance, B.; Saronio, C.; Leigh, J. S., Jr., *Proc. Natl. Acad. Sci. U.S.A.* **1975**, *72*, 1635–1640.
(11) Clore, G. M.; Andreasson, L. E.; Karlsson, B.; Aasa, R.; Malmström, B. G. *Biochem. J.* **1980**, *185*, 139–154.
(12) Clore, G. M.; Andreasson, L. E.; Karlsson, B.; Aasa, R.; Malmström, B. G. *Biochem. J.* **1980**, *185*, 155–167.
(13) Hansson, O.; Karlsson, B.; Aasa, R.; Vänngård, T.; Malmström, B. G. *EMBO J.* **1982**, *1*, 1295–1297.
(14) Blair, D. F.; Witt, S. N.; Chan, S. I. *J. Am. Chem. Soc.* **1985**, *107*, 7389–7399.
(15) Witt, S. N.; Chan, S. I. *J. Biol. Chem.* **1987**, *262*, 1446–1448.
(16) Spiro, T. G., Ed. *Biological Applications of Raman Spectroscopy*; Wiley and Sons: New York, 1987; Vol. 3.
(17) Kitagawa, T. In *Raman Spectroscopy of Biological Systems*; Clark, R. J. H., Hester, R. E., Eds.; 1986; pp 443–481.
(18) Hashimoto, S.; Tatsuno, Y.; Kitagawa, T. *Proc. Natl. Acad. Sci. U.S.A.* **1986**, *83*, 2417–2421.
(19) Sitter, A. J.; Reczek, C. M.; Terner, J. *J. Biol. Chem.* **1985**, *260*, 7515–7522.
(20) Bangcharoenpaurpong, O.; Rizos, A. K.; Champion, P. M.; Jollie, D.; Sligar, S. G. *J. Biol. Chem.* **1986**, *261*, 8089–8092.

0002-7863/93/1515-8527$04.00/0

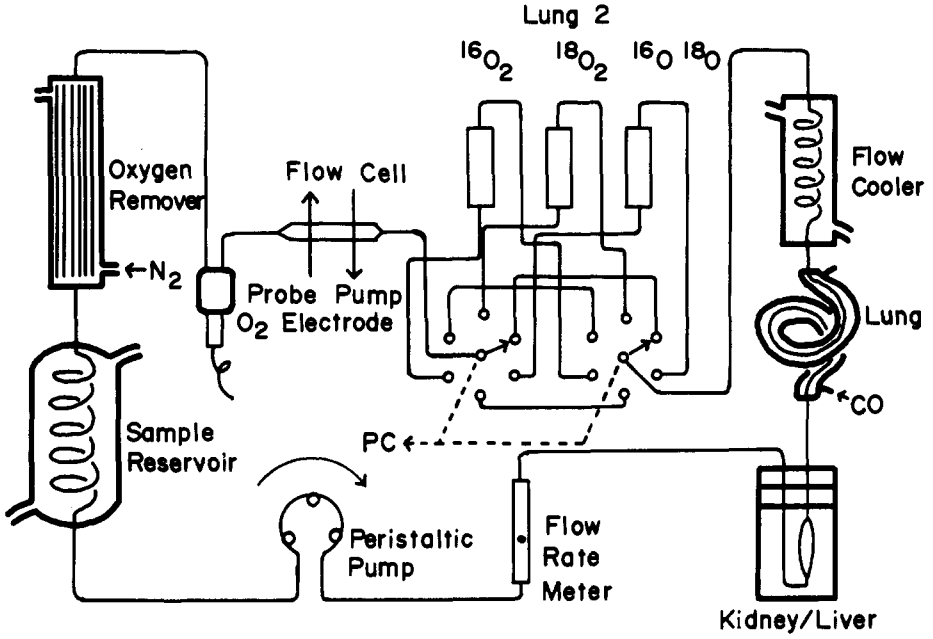

Figure 1. Improved artificial cardiovascular system for enzymatic reaction. Peristaltic pump: Cole Parmer, 7553–20. The "Kidney/Liver", Lung 1", "Lung 2", and "Flow Cooler" are essentially the same as those described previously.[31] The "Oxygen Remover" is improved, but see the text about its interpretation. A sample reservoir (100 mL) was incorporated into the improved device. Two six-directional rotary valves (Rheodyne, 5012) are simultaneously switched by an air actuator, which is controlled by a personal computer (PC) to select a particular lung containing suitable oxygen.

substantial information on the structure of CcO reaction intermediates, for which Ogura et al.[23] found an oxygen-isotope-sensitive band at 788 cm^{-1} and tentatively assigned it to the Fe^{IV}=O stretching mode ($\nu_{Fe=O}$) of the ferryl intermediate. The appearance of this band was confirmed by two other groups.[24,25] Unexpectedly, the 788-cm^{-1} band exhibited an upshift of ~14 cm^{-1} in D_2O,[25,26] although Varotsis and Babcock[24] noted insensitivity of the band to deuteration. This upshift could not be readily understood if one assumed a simple Fe^{IV}=O heme. In addition, Ogura et al. found another oxygen-isotope-sensitive band at 356 cm^{-1} whose time behavior appeared fairly similar to that of the 788-cm^{-1} band, and therefore they proposed an alternative assignment in which the bands at 788 and 356 cm^{-1} were attributed to the O–O and Fe–O stretching modes of the Fe^{III}–O–O–H group of the hydroperoxy intermediate.[26] To date there remain controversies concerning the assignment of the 788-cm^{-1} band. Furthermore, the rather broad and asymmetric band shape[26] suggested insufficient resolution for the Raman measurement. It is most critical to clarify the nature of this band in order to establish a reaction mechanism for dioxygen reduction. Accordingly, in this study we have reinvestigated the 788-cm^{-1} band with improved resolution under more well-defined and controlled conditions. We have succeeded in resolving the 788-cm^{-1} band into two bands which should arise from different intermediates, and we have assigned them to the hydroperoxy and ferryl intermediates on the basis of their temporal behavior, temperature dependence, and sensitivity to deuteration.

Experimental Procedures

CcO was isolated from bovine heart muscle according to the method described elsewhere.[27] It was stored in ice until use, with a typical concentration of 500 μM (in terms of heme *a*). The purified enzyme was typically used within 1–5 days but no later than 10 days after purification. Cytochrome *c* (Type IV) was purchased from Sigma and was used without further purification. D_2O and $^{18}O_2$ (98.2 atom %) were products of Showa Denko K.K. and ISOTEC, Inc., respectively. $^{16}O^{18}O$ was obtained by the Ce^{IV}-oxidation of $H^{16}O^{18}OH$, which was synthesized by reacting $H^{18}OF$ with $H_2{}^{16}O$.[28] The earlier procedure was improved by fluorinating $H^{18}OH$ in acetonitrile to obtain a solution of $H^{18}OF$ stabilized as a complex with CH_3CN.[29,30] The mass analysis of $^{16}O^{18}O$ gave $^{16}O^{18}O/^{16}O^{16}O/^{16}O^{17}O/^{17}O^{18}O/^{18}O^{18}O$ = 94:2.2:2.2:0.1:1.4. The sample solution for Raman experiments contained 100 μM CcO, 16.6 μM cytochrome *c*, and 50 mM ascorbate in 50 mM potassium phosphate buffer, pH 7.2. To replace the solvent H_2O with D_2O, the enzyme stock solution was concentrated to 2–3 mM, and 4 mL of the concentrated solution was diluted with 80 mL of D_2O (99.75%) buffer solution. The estimated concentration of the enzyme and deuterium enrichment in the D_2O solution are 100 μM and 95%, respectively.

About 80 mL of this solution was subjected to the Artificial Cardiovascular System (ACS), which has been significantly improved over the earlier version[31] and therefore is illustrated in Figure 1. The main changes include the following two parts: (1) The valves of lung 2 for introducing O_2 were replaced with two-channel synchronous valves driven by compressed N_2 gas, which were originally developed for liquid chromatography, so that they could be controlled by a computer through a built-in relay board. This replacement enabled us to observe the individual Raman spectra of intermediates derived from $^{16}O_2$, $^{18}O_2$, and $^{16}O^{18}O$ in turn and repeatedly and to accumulate the quasi-simultaneous spectra in computer memory. (2) The oxygen remover made from a glass tube was replaced with a highly efficient artificial lung originally produced for medical use (MERA, SILOX-S), in which many fine and very thin-skinned silicone tubes are bundled into a 20-cm-long cartridge. With this the surface area of the inner solution exposed to N_2 gas is as large as 0.3 m^2 for the volume of 20 mL. This lung allows the gas/liquid equilibrium to be reached in much less time than the previous oxygen remover and thus permits a higher flow speed. The flow cell used was of a quartz rectangular type (0.6 × 0.6 mm^2). The sample temperature was controlled by circulating water thermostatted at the specified

(21) Egawa, T.; Ogura, T.; Makino, R.; Ishimura, Y.; Kitagawa, T. *J. Biol. Chem.* **1991**, *266*, 10246–10248.
(22) Hu, S.; Schneider, A. J.; Kincaid, J. R. *J. Am. Chem. Soc.* **1991**, *113*, 4815–4822.
(23) Ogura, T.; Takahashi, S.; Shinzawa-Itoh, K.; Yoshikawa, S.; Kitagawa, T. *J. Biol. Chem.* **1990**, *265*, 14721–14723.
(24) Varotsis, C.; Babcock, G. T. *Biochemistry* **1990**, *29*, 7357–7362.
(25) Han, S.; Ching, Y.-c.; Rousseau, D. L. *Nature* **1990**, *348*, 89–90.
(26) Ogura, T.; Takahashi, S.; Shinzawa-Itoh, K.; Yoshikawa, S.; Kitagawa, T. *Bull. Chem. Soc. Jpn.* **1991**, *64*, 2901–2907.
(27) Yoshikawa, S.; Choc, M. G.; O'Toole, M. C.; Caughey, W. S. *J. Biol. Chem.* **1977**, *252*, 5498–5508.
(28) Appelman, E. H.; Thompson, R. C.; Engelkemeir, A. G. *Inorg. Chem.* **1979**, *18*, 909–911.
(29) Rozen, S.; Brand, M. *Angew. Chem., Int. Ed. Engl.* **1986**, *25*, 554–555.
(30) Appelman, E. H.; Dunkelberg, O.; Kol, M. *J. Fluorine Chem.* **1992**, *56*, 199–213.
(31) Ogura, T.; Yoshikawa, S.; Kitagawa, T. *Biochemistry* **1989**, *28*, 8022–8027.

temperature into the flow cooler of the ACS, while the temperature of the reservoir was maintained at 5 °C. The O_2 concentration after passages through the O_2 lung is 100–150 μM, which is appreciably lower than the concentrations used in the previously reported experiments.[7,8]

Raman scattering was excited at 423.0 nm; the exciting radiation was obtained from a dye laser (Spectra Physics 375B) with stilbene-420, pumped by an Ar^+ ion laser (Spectra Physics 2045) with 2-W total emission at 351.1–363.8 nm. The laser power at the flow cell was adjusted to be 10 mW unless otherwise stated. The beam diameter was 20 μm. For photodissociation of CO to initiate the reaction, another laser light (pump beam) was introduced and tuned to the α-band maximum of the Fe_{a3}–CO complex. Actually, the 590-nm output of a dye laser (Spectra Physics 375) with Rhodamine 6G was used. It was pumped by an Ar^+ ion laser (Spectra Physics 164) with total visible emission of 2.5 W. This pump beam was focused to 0.05 × 1 mm^2 at the cell by two cylindrical lenses, so that the beam could illuminate the entire cross-section of the flowing sample. The time-resolution of the Raman spectra is determined by the length of the pump beam along the flow direction (l_p) divided by the flow speed (l_p = 0.05 mm was determined by watching the laser beam with a microscope attached to the sample point). The laser power of the pump beam was made as high as 200 mW at the sample to achieve complete photodissociation of CO. The rise in temperature by laser illumination under the present conditions was negligible; 0.2 J/s for the sample flowing 40 mL/min would be expected to raise the temperature by 0.2 °C even if 100% of the photon energy were absorbed by the solution.

Raman-scattered radiation was collected with a microscope objective lens (NA = 0.25) and focused onto the entrance slit of a monochromator by an achromatic lens (f = 150 mm) after passing through a filter with a short-wavelength cutoff at 420 nm. This system for collection of Raman-scattered light has a better spatial resolution than a camera lens system and, therefore, results in less disturbance from the nearby pump beam. Use was made of a single monochromator (Ritsu Oyo Kogaku, DG-1000) newly constructed for this study. The focal length of the spectrometer was 1000 mm, and it has two interchangeable blazed holographic gratings (500 nm, 1200 grooves/mm, and 900 nm, 1200 grooves/mm). These gratings were used at the first- and second-order geometry for normal (~1.0 cm^{-1}/channel) and higher resolutions (~0.4 cm^{-1}/channel), respectively. The dispersed light was detected with an intensified photodiode array cooled to −20 °C (Princeton Applied Research, 1421HQ). Sensitivity variations of individual channels of the detector and the wavelength dependence of the transmittance of the cutoff filter were corrected by dividing the raw Raman spectrum by a white-light spectrum. No other corrections were made to the observed spectra in this study. Raman frequencies were calibrated with Raman bands of ethyl alcohol injected into the flow cell soon after the sample measurements without any geometrical changes in the sample illumination system. Raman frequencies of ethanol were separately calibrated with indene as a standard. The wavenumber accuracy was ±2 and ±4 cm^{-1} for intense and weak Raman bands, respectively, measured at normal resolution.

Results

Figure 2 depicts the TR^3 spectra of CO-bound CcO. Spectra A and B were obtained with 0.5-mW probe power under anaerobic conditions in the absence and presence of the pump beam, respectively, while spectrum C was obtained with a 200-mW pump beam and a 10-mW probe beam in the presence of O_2. In spectrum A there are two bands, at 575 and 517 cm^{-1}, which are assigned respectively to the Fe–C–O bending (δ_{Fe-C-O}) and the Fe–CO stretching (ν_{Fe-CO}) of the Fe_{a3}^{II}–CO complex[32,33] on the basis of the ^{13}C and ^{18}O isotopic frequency shifts of CO. The bands at 750, 683, and 342 cm^{-1}, on the other hand, arise from heme *a* vibrations (ν_{16}, ν_7, and ν_8, respectively). The Raman bands associated with CO were depleted upon introduction of the pump beam (Δt = 0.5 ms), as is evident in spectrum B, reflecting complete photodissociation under these experimental conditions. Moreover, reduction in intensity of the porphyrin ν_{16}, ν_7, and ν_8 modes is consistent with the shift of the absorption maximum of cytochrome a_3 from 430 to 442 nm upon conversion from the CO-bound to the CO-dissociated form. This fact also suggests

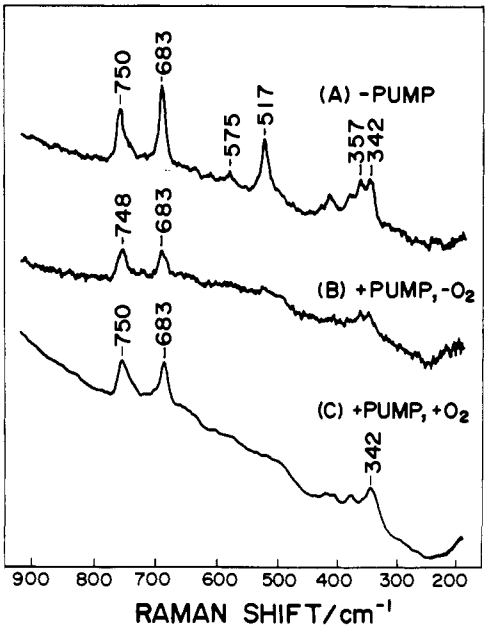

Figure 2. Time-resolved resonance Raman spectra of CO-bound cytochrome *c* oxidase for Δt = 0.5 ms at 5 °C: (A) in the absence of the pump beam under anaerobic conditions, *i.e.* the probe-only spectrum; (B) in the presence of the pump beam under anaerobic conditions; (C) in the presence of the pump beam under aerobic conditions. The ordinate scale is common to A and B. Experimental conditions: probe beam, 0.5 mW for A and B and 10 mW for C at 423.0 nm; pump beam, 220 mW at 590.0 nm; accumulation time, 80 s for A and B and 320 s for C.

that the excitation wavelength of 423.0 nm used in this experiment is appropriate for probing reaction intermediates that are expected to have absorption maxima closer to that of the CO-bound form than to that of the CO-dissociated form. Spectrum C in Figure 2, obtained with the pump beam in the presence of O_2, is expected to contain the contributions from reaction intermediates at Δt = 0.5 ms. Longer accumulation time for spectrum C yields signal-to-noise (S/N) ratio higher than that in spectra A and B. However, since Raman bands associated with the heme-bound oxygen are so weak, the presence of the Fe^{II}–O_2 stretching band (ν_{Fe-O2}) is not obvious in this raw spectrum. The oxygen-isotope-sensitive bands could be clearly identified when difference spectra ($^{16}O_2$ minus $^{18}O_2$) were calculated. Accordingly, such difference spectra will be presented hereafter as the TR^3 spectra. All the TR^3 measurements were carried out under identical optical conditions except for variations of the delay time (Δt) and temperature.

The left side of Figure 3 depicts the TR^3 difference spectra at Δt = 0.1 ms which were obtained after intensity normalization of individual spectra by the 683-cm^{-1} band (see Figure 2): (A) $^{16}O_2$–$^{18}O_2$; (B) $^{16}O^{18}O$–$^{18}O_2$; (C) $^{16}O_2$–$^{16}O^{18}O$; and (D) $^{16}O^{18}O$–($^{16}O_2$+$^{18}O_2$)/2. Spectrum A reproduces well the difference spectra reported so far.[34-36] The simultaneously observed absorption spectrum implicated compound A, which has been demonstrated to be the first intermediate by cryogenic absorption spectroscopy.[9] The band at 571 cm^{-1} was assigned to the ν_{Fe-O2} mode of the dioxy complex. Spectrum B suggests a slight downshift of the 571-cm^{-1} positive peak for $^{16}O_2$ to 569 cm^{-1} for $^{16}O^{18}O$ but no shift for the 544-cm^{-1} negative peak. Similarly, comparison of spectrum A with spectrum C shows a slight upshift of the negative band at 544 cm^{-1} for $^{18}O_2$ to 548 cm^{-1} for $^{16}O^{18}O$ but no shift for the positive peak at 571 cm^{-1}. Spectrum D was

(32) Argade, P. V.; Ching, Y.-c.; Rousseau, D. L. *Science* **1984**, *225*, 329–331.

(33) Hirota, S.; Ogura, T.; Shinzawa-Itoh, K.; Yoshikawa, S.; Kitagawa, T. To be published.

(34) (a) Varotsis, C.; Woodruff, W. H.; Babcock, G. T. *J. Am. Chem. Soc.* **1989**, *111*, 6439–6440. (b) Varotsis, C.; Woodruff, W. H.; Babcock, G. T. *J. Am. Chem. Soc.* **1990**, *112*, 1297.

(35) Ogura, T.; Takahashi, S.; Shinzawa-Itoh, K.; Yoshikawa, S.; Kitagawa, T. *J. Am. Chem. Soc.* **1990**, *112*, 5630–5631.

(36) Han, S.; Ching, Y.-c.; Rousseau, D. L. *Proc. Natl. Acad. Sci. U.S.A.* **1990**, *87*, 2491–2495.

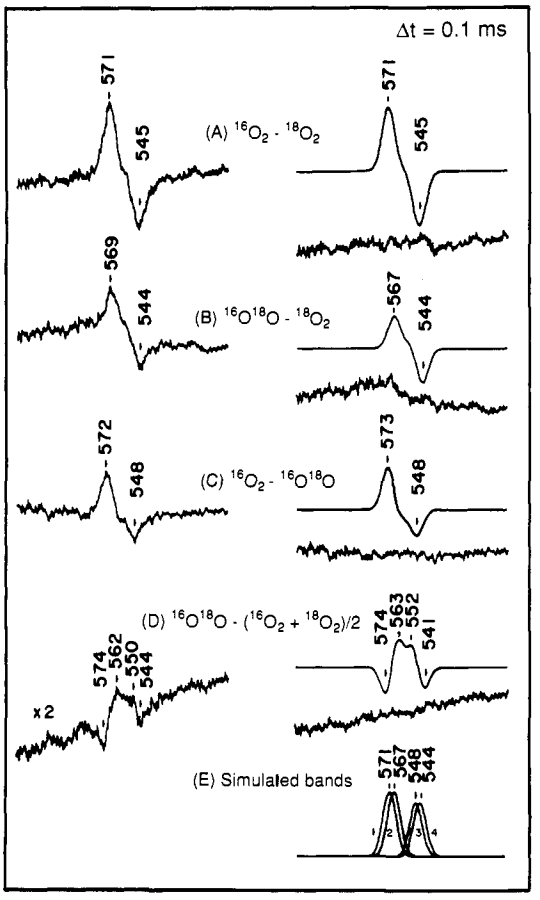

Figure 3. Time-resolved resonance Raman difference spectra in the Fe^{II}–O_2 stretching frequency region of cytochrome *c* oxidase at Δt = 0.1 ms: (left side) observed spectra; (right side) calculated spectra; (A) $^{16}O_2$ – $^{18}O_2$; (B) $^{16}O^{18}O$ – $^{18}O_2$; (C) $^{16}O_2$ – $^{16}O^{18}O$; (D) $^{16}O^{18}O$ – ($^{16}O_2$ + $^{18}O_2$)/2. (E) Fe–$^{16}O_2$ (1), Fe–$^{16}O^{18}O$ (2), Fe–$^{18}O^{16}O$ (3), and Fe–$^{18}O_2$ (4) stretching Raman bands assumed in the simulation. The peak intensity ratios are 6:6:5:5, and all have the Gaussian band shape with a FWHM of 12.9 cm^{-1}. In the calculation for the $^{16}O^{18}O$ spectrum, (spectrum 2 + spectrum 3)/2 was used. The differences between the observed and calculated spectra are depicted with the same ordinate scale as that of the observed spectra under the individual calculated spectra. Experimental conditions: probe beam, 423.0 nm, 4 mW; pump beam, 590 nm, 210 mW; accumulation time, 4800 s.

obtained by subtraction of [(spectrum for $^{16}O_2$ + spectrum for $^{18}O_2$)/2] from the spectrum for $^{16}O^{18}O$. It appeared that there are two negative peaks at ~574 and ~544 cm^{-1} and two positive peaks around 562 and 550 cm^{-1}.

Since the peak positions in the difference spectra do not always indicate the peak positions in each raw spectrum when two bands are fairly close, we carried out simulation calculations by assuming a Gaussian band-shape, and the results are illustrated on the right side of Figure 3. The band intensities and positions of the Fe–O_2 stretching bands for the Fe–$^{16}O_2$, Fe^{16}–O^{18}O, Fe–$^{18}O^{16}O$, and Fe–$^{18}O_2$ complexes were assumed as shown by spectrum 1 (571 cm^{-1}), spectrum 2 (567 cm^{-1}), spectrum 3 (548 cm^{-1}), and spectrum 4 (544 cm^{-1}) of Figure 3E, respectively, and their peak intensity ratios were 6:6:5:5 with the same full-width of 12.9 cm^{-1}. The difference spectrum, spectrum 1 – spectrum 4, is depicted at the right side of part A, and the difference between the left spectrum and the right spectrum is depicted with the same scale as that of the left spectrum under the calculated spectrum on the right side. The calculated difference spectrum shown by Figure 3A well reproduces the observed spectrum. Similarly, right spectrum B was obtained as (spectrum 2 + spectrum 3)/2 – spectrum 4, and right spectrum C as spectrum

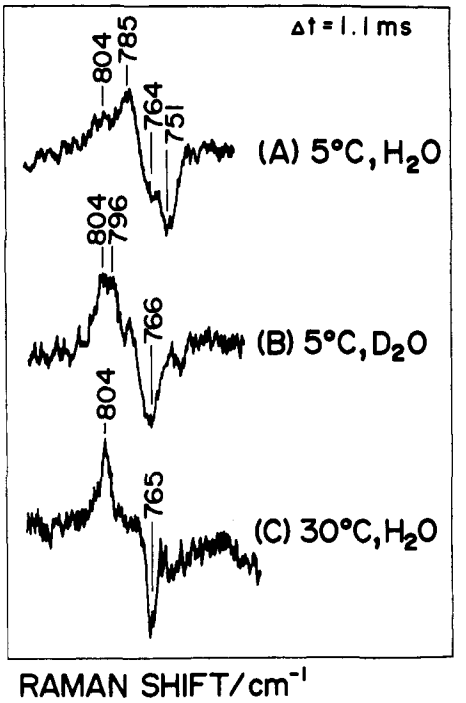

Figure 4. Higher resolution time-resolved resonance Raman difference spectra ($^{16}O_2$ – $^{18}O_2$) in the ~800-cm^{-1} region of cytochrome *c* oxidase at Δt = 1.1 ms: (A) 5 °C in H_2O; (B) 5 °C in D_2O; (C) 30 °C in H_2O. Resolution, 0.43 cm^{-1}/channel (450 points plotted). Accumulation time, 14220, 2700, and 540 s for A, B, and C, respectively.

1 – (spectrum 2 + spectrum 3)/2. Since right spectrum D represents the difference, (spectrum 2 + spectrum 3) – (spectrum 1 + spectrum 4), left spectrum D is expanded by a factor of 2 more than defined. There are no residual features in the experimental minus calculated difference spectrum of Figure 3D, demonstrating that the simulation is quite satisfactory and that the bands assumed by Figure 3E are realistic. The presence of two Fe–O_2 stretching bands for the $^{16}O^{18}O$ adduct conclusively indicates that two oxygen atoms of dioxygen are not equivalent as seen for oxyHb[37] and oxyhemerythrin (oxyHr),[38] namely, the formation of an end-on-type dioxygen complex as the first intermediate.

In the previous low-resolution TR[3] difference spectra for Δt = 0.4–2.2 ms,[26] the positive peak around 788 cm^{-1} appeared as if it were a doublet, although the S/N ratio was not high enough to permit assignment of the positions of the two component peaks. Therefore an average frequency was labeled. In the present study the high-resolution experiments were carried out with a focus on this band. Figure 4 depicts the TR[3] difference spectra ($^{16}O_2$ minus $^{18}O_2$) obtained at Δt = 1.1 ms for different sample conditions as specified for the individual spectra. The higher resolution condition (approximately 0.43 cm^{-1}/channel) does not allow the simultaneous observation of the frequency region near the other oxygen-isotope-sensitive band at 356 cm^{-1}. As seen in spectrum A, there are bands at 804 and 785 cm^{-1} for $^{16}O_2$, and they show downshifts to 764 and 751 cm^{-1}, respectively, for $^{18}O_2$. Thus, the doublet has been confirmed without doubt under the higher resolution condition. It is evident in spectrum B that only the $^{16}O_2$/$^{18}O_2$ band pair at 785/751 cm^{-1} in H_2O shows an upshift to 796/766 cm^{-1} in D_2O. Since the 785/751-cm^{-1} pair in spectrum A is more intense than the 804/764-cm^{-1} pair, the apparent upshift from 788 to 802 cm^{-1} is a reasonable description of the previous results at low-resolution.[25,26] The presence of bands at 804 and 796 cm^{-1} in D_2O (spectrum B) was repeatedly confirmed for

(37) Duff, L. L.; Appelman, E. H.; Shriver, D. F.; Klotz, I. M. *Biochem. Biophys. Res. Commun.* **1979**, *90*, 1098–1103.
(38) Kurtz, D. M., Jr.; Shriver, D. F.; Klotz, I. M. *Coord. Chem. Rev.* **1977**, *24*, 145–178.

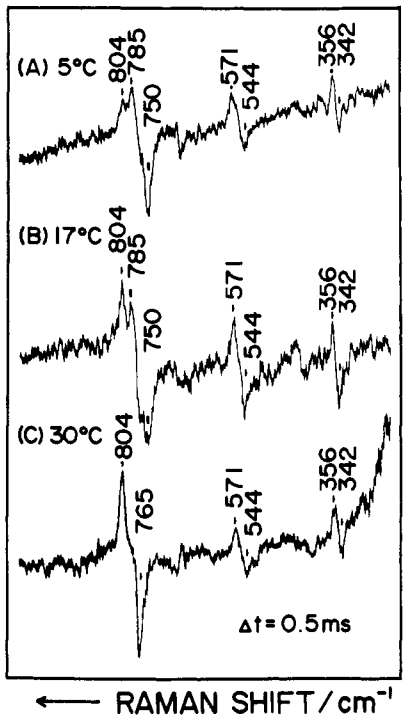

Figure 5. Time-resolved resonance Raman difference spectra ($^{16}O_2$ – $^{18}O_2$) of cytochrome *c* oxidase in H_2O at Δt = 0.5 ms: (A) 5 °C; (B) 17 °C; (C) 30 °C. Resolution, 1 cm^{-1}/channel.

different preparations of the sample, although their relative intensity was somewhat variable from one experiment to another. This fact indicates that the previously detected broad feature centered at 800 cm^{-1} for the D_2O solution[25,26] is not a consequence of a single band but of two overlapping bands with slightly different frequencies (804 and 796 cm^{-1}). The $^{16}O_2/^{18}O_2$ band pair at 785/751 cm^{-1} loses its intensity at 30 °C, as seen in spectrum C, while the band pair at 804/765 cm^{-1} remains. This band pair increased in intensity with increase of the delay time from Δt = 0.1 to 1.1 ms at 30 °C, but its shape was not altered between Δt = 0.1 and 1.1 ms. The 804/765-cm^{-1} band pair at 30 °C exhibited no frequency shift in D_2O (not shown); this was also the case at 5 °C. These features were essentially the same for Δt = 0.5 ms (not shown). Consequently, the present experiments confirmed that the previously observed band at 788 cm^{-1} at 5 °C in H_2O was actually composed of two overlapping bands at 804 and 785 cm^{-1} and that these two bands arose from different reaction intermediates.

In order to see if other oxygen-isotope-sensitive bands at 571 and 356 cm^{-1} also exhibit some temperature dependence similar to that of the 804/785-cm^{-1} pair, the TR[3] experiments under normal resolution (approximately 1.0 cm^{-1}/channel) were carried out at different temperatures. The results are shown in Figure 5, where the temperature is specified on the left of each spectrum. As evident in spectra A and B, the bands at 804 and 785 cm^{-1} are clearly resolved even under normal resolution, but we were not confident of such splitting without the higher resolution data shown in Figure 4. The relative intensities of the 785- and 804-cm^{-1} bands (I_{785}/I_{804}) are reversed between 5 and 17 °C, while the former disappears at 30 °C. On the other hand, the ratio of intensities of the bands at 804 and 356 cm^{-1} (I_{356}/I_{804}) is almost unity at 5 °C, 0.8 at 17 °C, and 0.2 at 30 °C.

The band at 450 cm^{-1}, which was recognized in the previous TR[3] spectrum observed at 5 °C for Δt = 2.2 ms and assigned to the Fe^{III}–OH stretching mode of the Fe^{III}–OH intermediate,[25,26] was not clearly observed at 30 °C in spectrum C (Δt = 0.5 ms) or for Δt = 2.2 ms (not shown), suggesting a faster exchange of the hydroxy ligand of the Fe^{III}–OH intermediate with bulk water. It is noted that the band at 356 cm^{-1} is still observable at 30 °C,

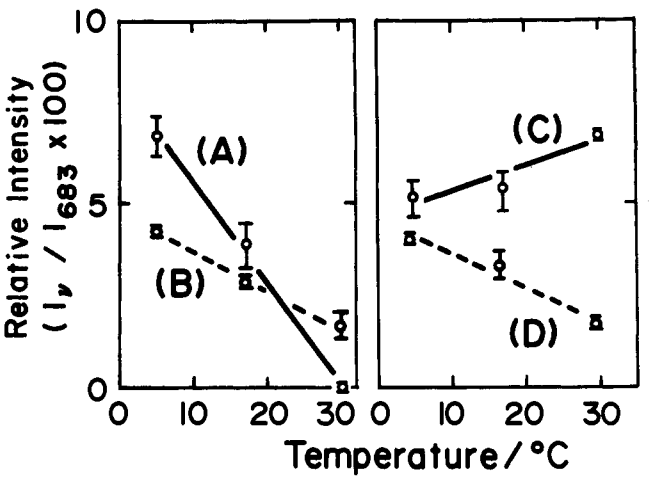

Figure 6. Temperature dependence of the intensities of the Oxygen-isotope-sensitive Raman bands. The valley-to-peak intensity differences in the difference spectra (Figure 5) relative to the intensity of the porphyrin band at 683 cm^{-1} in the original spectra are plotted against temperature. The solid lines and broken lines are drawn for easy viewing: (A) 785 cm^{-1}; (B) 356 cm^{-1}; (C) 804 cm^{-1}; (D) 571 cm^{-1}.

although that at 785 cm^{-1} is not. These observations definitely indicate that the bands at 785 and 356 cm^{-1} originate from different intermediates, contrary to our previous report.[26]

To examine the temperature dependence quantitatively, the intensities of the oxygen-isotope-sensitive bands at 356, 571, 785, and 804 cm^{-1} in the spectra for Δt = 0.5 ms were determined with respect to the intensity of the porphyrin ν_7 mode at 683 cm^{-1} and are plotted against temperature in Figure 6. Although the temperature-dependent intensity changes of the bands at 356 (Figure 6B) and 571 cm^{-1} (Figure 6D) are apparently alike, their variations with time are quite distinct at 5 °C,[26] and they are therefore assigned to different species. The band at 785 cm^{-1} (Figure 6A) becomes weaker as the temperature rises and disappears altogether at 30 °C, while the band at 804 cm^{-1} (Figure 6C) seems to become rather stronger at higher temperatures. Therefore, the 804- and 785-cm^{-1} bands must also arise from different species.

The Fe^{4+}=O stretching vibration ($\nu_{Fe=O}$) of the ferryl intermediate and the O—O stretching vibration (ν_{O-O}) of the peroxy intermediate are expected to have similar frequencies around 750–850 cm^{-1}. These two modes cannot be distinguished by the $^{16}O_2$ and $^{18}O_2$ isotopic frequency shifts. However, if $^{16}O^{18}O$ is used to produce such intermediates, the peroxy intermediate is expected to give a band at a frequency intermediate between those for the $^{16}O_2$ and $^{18}O_2$ derivatives.[36] In contrast, the ferryl intermediate for $^{16}O^{18}O$ is expected to yield two bands at the same frequencies as those seen for the $^{16}O_2$ and $^{18}O_2$ derivatives but with half their intensity. In fact such distinguishment was satisfactorily carried out with $^{16}O^{18}O$ for *Escherichia coli* cytochrome *d*.[39] Accordingly, we examined the effect of $^{16}O^{18}O$ on the 804- and 785-cm^{-1} bands. In this experiment, Raman scattering from the reaction intermediates formed with $^{16}O_2$, $^{18}O_2$, and $^{16}O^{18}O$ was observed in turn under higher resolution at 8-min intervals by switching the two valves of Lung 2 illustrated in Figure 1. The difference spectrum between the oxygen isotopes could be made precise by these quasi-simultaneous measurements of three isotopes. The results are depicted in Figure 7, where the TR[3] difference spectra obtained in the H_2O and D_2O solutions for the combinations defined at the center of the figure are presented on the left and right sides, respectively. The order of spectral dispositions is the same between Figures 3(left) and 7, but their appearances are distinct.

(39) Kahlow, M. A.; Zuberi, T. M.; Gennis, R.-B.; Loehr, T. M. *Biochemistry* **1991**, *30*, 11485–11489.

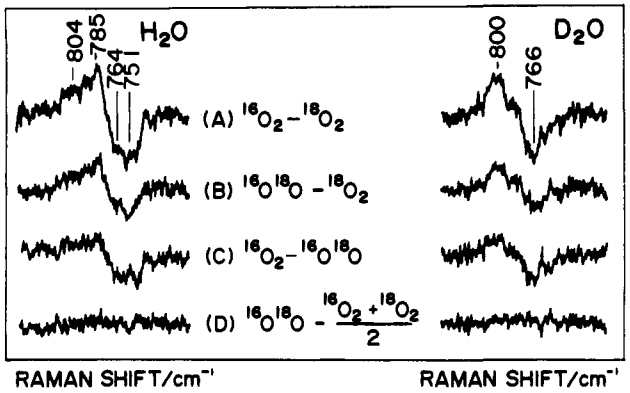

Figure 7. Higher resolution time-resolved resonance Raman difference spectra of cytochrome *c* oxidase in the ~800-cm^{-1} region for Δt = 1.1 ms at 5 °C for H_2O (left) and D_2O solutions (right). The ordinate scales are common to all spectra. The spectra combined in the difference calculations are specified in the middle of the figure. Resolution, 0.43 cm^{-1}/channel.

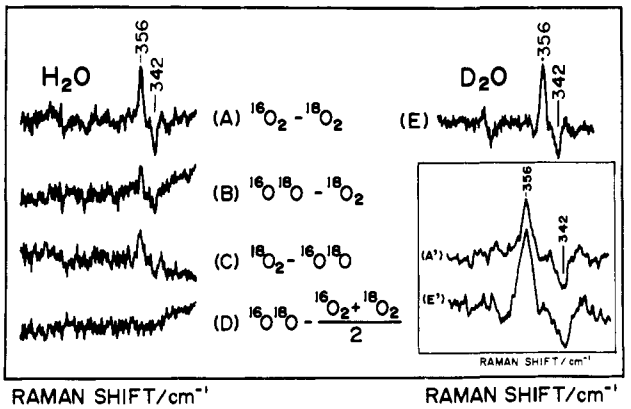

Figure 8. Time-resolved resonance Raman difference spectra of cytochrome *c* oxidase in the ~350-cm^{-1} region for Δt = 0.5 ms at 5 °C for H_2O (left) and D_2O solutions (right). The ordinate scales are common to all spectra. The spectra combined in the difference calculations are specified in the middle of the figure. The inset depicts the plots of spectra A and E expanded by a factor of 2.5 in the wavenumber axis.

The top spectra in Figure 7 (spectra A) were obtained under the same conditions as spectra A and B in Figure 4. In the left spectrum A for the H_2O solution, there are bands at 804 and 785 cm^{-1} for $^{16}O_2$, and they show downshifts to 764 and 751 cm^{-1} for $^{18}O_2$, in agreement with the results of Figure 4A. Similarly, for the D_2O solution, there are the overlapping bands around 800 cm^{-1} (peaks are 804 and 796 cm^{-1}) for $^{16}O_2$ and around 766 cm^{-1} for $^{18}O_2$. These results confirm reproducibility of the data for independent experiments with different batches of the enzyme preparations. It is evident that the peak positions and spectral patterns of the difference spectra B and C in Figure 7 for the H_2O solution are alike and are similar to those of spectrum A but that their intensities are only approximately half those in spectrum A. The same features are also seen for the D_2O solution (right side). The point to be emphasized is that there is no difference peak in the bottom traces for either the H_2O or the D_2O solutions. This feature definitely differs from that seen in Figure 3D. These results indicate that only one atom of O_2 is primarily responsible for the two RR bands. In other words, neither of the bands at 804 and 785 cm^{-1} is assignable to the O–O stretching mode.

In order to see any $^{16}O^{18}O$ effect on the band at 356 cm^{-1}, we repeated the $^{16}O^{18}O$ experiment for the low-frequency region, since the bands at 804–785 and 356 cm^{-1} could not be covered simultaneously under the higher resolution conditions. Figure 8 depicts the TR^3 difference spectra. Spectra A–D were obtained from the combinations of O_2 isotopes in the H_2O solution as designated for each spectrum, while spectrum E was obtained from combination A for the D_2O solution. It is evident that there is no deuteration effect on the absolute frequency of the bands at 356/342 cm^{-1}, in agreement with the previous observation.[26] As was seen for the 804/785-cm^{-1} doublet, spectra B and C do not differ from each other in shape or position of the peaks, which are close to those of spectrum A. Furthermore, as in Figure 7D, there is no difference peak in spectrum D of Figure 8. Accordingly, it became clear again that only one atom of the O_2 molecule is primarily responsible for the 356-cm^{-1} band.

Table I. Observed Frequencies of Oxygen-Isotope-Sensitive Bands for Reaction Intermediates of Cytochrome *c* Oxidase (cm^{-1})

	H_2O			D_2O		
possible species	$^{16}O_2$	$^{16}O^{18}O$	$^{18}O_2$	$^{16}O_2$	$^{16}O^{18}O$	$^{18}O_2$
Fe^{IV}=O	804	804, 765	765	804	804, 765	765
Fe^{III}—O—O—H	785	785, 751	751	796	796, 766	766
Fe^{II}—O_2	571	567, 548	544	571		544
Fe^{III}—OH	450		425	443		415
?	356	356, 342	342	356	356, 342	342

Spectra in Figures 7 and 8 are drawn on the same wavenumber scale, and the 356-cm^{-1} band is seen to be very narrow. The inset of Figure 8 (spectra A′ and E′) shows plots of spectra A and E with the wavenumber axis expanded by 2.5-fold. The 356-cm^{-1} band appears to be somewhat broader in D_2O than in H_2O, but both spectra exhibit a flat region between the positive and negative peaks. This means that the separation between the $^{16}O_2$ and $^{18}O_2$ peaks is larger than their bandwidths, and thus the narrowness of the band is not the consequence of the close proximity of the $^{16}O_2$ and $^{18}O_2$ bands. This also means that the peak positions of the difference spectrum correctly represent those of each rough spectrum. If the bandwidth depends on the conformational inhomogeneity, the narrow band may suggest compact packing of amino acid residues around the bound oxygen at the catalytic site in this reaction intermediate. For convenience sake, the frequencies of all the oxygen-isotope-sensitive bands of reaction intermediates of CcO observed in our studies are summarized in Table I.

Discussion

End-On-Type Oxy Complex. The Fe–O_2 stretching Raman band has been observed at 567–572 cm^{-1} for oxyhemoglobin (oxyHb)[40,41] and oxyMb.[42] For the former, the corresponding band[37] for pure $^{16}O^{18}O$ appeared as two bands. The X-ray crystallographic analysis for oxyHb[43] demonstrated the end-on binding to the heme iron. The Fe–O_2H stretching band of oxyHr[38] also displayed two bands at 502 and 484 cm^{-1} for $^{16}O^{18}O$ in contrast with a single band at 504 cm^{-1} for $^{16}O_2$ and at 482 cm^{-1} for $^{18}O_2$, and its end-on binding to the Fe^{II} ion was confirmed by X-ray crystallography.[44] Simulation calculations for the results shown in Figure 3(left) suggested the presence of the corresponding bands of CcO at 571 cm^{-1} for $^{16}O_2$, 567 and 548 cm^{-1} for $^{16}O^{18}O$, and 544 cm^{-1} for $^{18}O_2$. If it were a side-on complex, the $^{16}O^{18}O$ derivative should have given rise to a single sharp Fe–O_2 stretching band. Consequently, the present experiments conclusively demonstrate that the first intermediate of CcO is an end-on-type dioxygen adduct.

In contrast with the similarity of the ν_{Fe-O2} frequency of CcO (571 cm^{-1}) to those of oxyHb[40,41] and oxyMb,[42] the Fe–CO stretching frequency of the CO adduct of CcO (CcO·CO), which is located around 517–522 cm^{-1},[32,33] is distinctly higher than those

(40) Brunner, H. *Naturwissenschaften* **1974**, *61*, 129.
(41) Nagai, K.; Kitagawa, T.; Morimoto, H. *J. Mol. Biol.* **1980**, *136*, 271–289.
(42) Van Vart, H. E.; Zimmer, J. *J. Biol. Chem.* **1985**, *260*, 8372–8377.
(43) Shaanan, B. J. *J. Mol. Biol.* **1983**, *171*, 31–59.
(44) Holmes, M. A.; Trong, I. L.; Turley, S.; Sieber, L. C.; Stenkamp, R. E. *J. Mol. Biol.* **1991**, *218*, 583–593.

Chart I. Possible Structures of 2- and 3-Electron-Reduced Reaction Intermediates

Structure I	Structure II	Structure III
Fe^{3+}-O-O-H	Fe^{3+}-O-O-Cu^{2+}	
Structure IV	**Structure V**	**Structure VI**
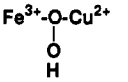	Fe^{4+}=O	Fe^{4+}=O(Por)$^{\cdot+}$

of HbCO and MbCO (507–512 cm^{-1}).[45] The reason for the difference is not clear at the present stage but may be related to the difference of steric effects caused by surrounding amino acid residues on CO and O_2.

Assignments of the Bands at 804 and 785 cm^{-1}. The present study has revealed the presence of bands at 804 and 785 cm^{-1} for Δt = 1.1 ms at 5 °C, although earlier results have suggested the presence of only one band at 788 cm^{-1} and have given rise to some controversy about its assignment. Here we propose new assignments, but before explaining them, we will first summarize the discussions to date. Chart I illustrates possible structures of the reaction intermediates to which the two bands in question could be assigned. If one takes into consideration only the absolute frequency and its shift upon $^{18}O_2$ substitution, plausible candidates for vibrational modes to which Raman bands around 800 cm^{-1} could be assigned are the ν_{OO} of a peroxo (O_2^{2-}, structures I–IV)[46] and the $\nu_{Fe=O}$ of a ferryl intermediate (structures V and VI).

As to the 788-cm^{-1} band of CcO, Han *et al.*[25] assumed structure V and explained the high-frequency shift of $\nu_{Fe=O}$ in D_2O as a result of the oxygen atom bound to the heme iron being hydrogen bonded in H_2O but not in D_2O. This interpretation postulates a large conformational change of the protein upon deuteration. If such a large structural change as disruption of the hydrogen bond occurs, it should result in quite different reaction kinetics in D_2O. Although the kinetics are not strictly the same between H_2O and D_2O,[47] the differences revealed by time-resolved RR measurements[26] are small, and this leads us to infer that such a large conformational change is unlikely.

On the other hand, Ogura *et al.* assumed the Fe^{III}–O–O–H structure[26] (structure I) and assigned the band at 788 cm^{-1} to the ν_{OO} mode, since they did not have the data for $^{16}O^{18}O$. They found another band with oxygen-isotope sensitivity at 356 cm^{-1}, which downshifted to 342 cm^{-1} upon $^{18}O_2$ substitution. This band was insensitive to deuteration. The time dependences of the 788- and 356-cm^{-1} bands were apparently alike, as though they had arisen from an identical intermediate. Since the Fe^{IV}=O heme should give only one oxygen-isotope-sensitive RR band (the Fe^{IV}=O bending mode is expected to be infrared active but not Raman active under the C_{4v} symmetry), Ogura *et al.* suggested that most probably the bands at 788 and 356 cm^{-1} arose from the ν_{OO} and ν_{Fe-O} modes of the Fe^{III}–O–O–H group. For oxyHr with structure I,[38] the band for $^{16}O_2$ at 844 cm^{-1} showed a downshift to 822 and 798 cm^{-1} upon $^{16}O^{18}O$ and $^{18}O_2$ substitution, respectively. The ν_{OO} bands of oxyHr[48] and hydrogen peroxide[49] exhibit an upshift by ~4 cm^{-1} upon deuteration. Accordingly, the assignment of the 785-cm^{-1} band to ν_{OO} seemed plausible.[26] However, the experimental results using $^{16}O^{18}O$ shown in Figure 7 could not validate this assignment.

Since this is the first paper to note the presence of two bands near 800 cm^{-1}, the characteristics of these bands are summarized first. The nature of the band at 804 cm^{-1} is as follows: (1) It shows a downshift by 40 cm^{-1} upon $^{18}O_2$ substitution both at 5 °C and 30 °C. (2) It shows little frequency shift in D_2O either at 5 °C or at 30 °C. (3) Experiments using $^{16}O^{18}O$ reveal that only one oxygen atom of dioxygen primarily determines the vibrational frequency. The nature of the band at 785 cm^{-1} is as follows: (1) It shows a downshift by 34 cm^{-1} upon $^{18}O_2$ substitution at 5 °C. (2) It shows an upshift by 11 cm^{-1} in D_2O at 5 °C. (3) It loses Raman intensity at 30 °C. (4) Similar to the case of the band at 804 cm^{-1}, the vibrational frequency depends primarily on one oxygen atom of dioxygen.

If a ferryl porphyrin π-cation radical (structure VI in Chart I) coexists with the neutral ferryl complex, two $\nu_{Fe=O}$ bands may be observed in the 800-cm^{-1} region.[50-54] However, the time-resolved RR spectra of CcO in the higher frequency region[24,55] do not suggest the coexistence of the π-cation radical with the neutral ferryl complex. If there were two neutral ferryl intermediates in which one is hydrogen bonded and the other is not, the deuteration sensitivity might be different between the two $\nu_{Fe=O}$ modes. However, the upshift by 11 cm^{-1} upon deuteration seems too large to be ascribed to a difference between hydrogen and deuterium bonds.

Structure IV was once proposed for an intermediate of CcO,[56] but such a small distance between the Fe_{a3} and Cu_B ions contradicts the recent IR observations[57] that the vibrational frequencies of the external ligands (L) such as CN^- and N_3^- in a double-coordinated complex (Fe_{a3}–L, Cu_B–L) were identical with those found in a single-coordinated one (Fe_{a3}–L, Cu_B) and (Fe_{a3}, Cu_B–L). We therefore exclude the possibility of structure IV.

The upshift of the 785-cm^{-1} band upon deuteration limits plausible models to structure I. The question to be answered is whether structure I can explain all the observations satisfactorily. We therefore carried out normal coordinate calculations for an isolated Fe–O–O–H molecule according to the standard GF-matrix method.[58] The assumed potential function (V) is of a Urey–Bradley–Shimanouchi type as represented by

$$2V = K_{FeO}(\Delta r_{Fe-O})^2 + K_{OO}(\Delta r_{OO})^2 + K_{OH}(\Delta r_{OH})^2 + H_{FeOO}(\Delta\delta_{FeOO})^2 + H_{OOH}(\Delta\delta_{OOH})^2 + F_1(\Delta q_{Fe\,O})^2 + F_2(\Delta q_{O\,H})^2 + P(\Delta\tau)^2$$

where Δr_i, $\Delta\delta_i$, Δq_i, and $\Delta\tau$ are the stretching, bending, nonbonding repulsion, and torsion coordinates, respectively, and K_i, H_i, F_i, and P are their harmonic force constants. Since the purpose of this calculation is to see whether the observed results can be explained within the framework assumed above, the force constants were appropriately adjusted. The values of the potential parameters used and the calculated results are summarized in Table II.

The ν_{Fe-O} mode is calculated to be at 787 cm^{-1}, shifting up to 798 cm^{-1} for the deuterated form and down to 749 cm^{-1} for the $^{18}O_2$ derivative. The corresponding frequencies for the $^{16}O^{18}O$ derivative are calculated to be 782 and 753 cm^{-1} for Fe–O–O–H

(45) Tsubaki, M.; Srivastava, R. B.; Yu, N.-T. *Biochemistry* **1982**, *21*, 1132–1140.
(46) McCandish, E.; Miksztal, A. R.; Nappa, M.; Sprenger, A. Q.; Valentine, J. S.; Stong, J. D.; Spiro, T. G. *J. Am. Chem. Soc.* **1980**, *102*, 4268–4271.
(47) Thörnström, P.-E.; Soussi, B.; Arvidsson, L.; Malmström, B. G. *Chem. Scr.* **1984**, *24*, 230–235.
(48) Shiemke, A. K.; Loehr, T. M.; Sanders-Loehr, J. *J. Am. Chem. Soc.* **1984**, *106*, 4951–4956.
(49) Giguere, P. A.; Srinivasan, T. K. K. *J. Raman Spectrosc.* **1974**, *2*, 125–132.
(50) Salehi, A.; Oertling, W. A.; Babcock, G. T.; Chang, C. K. *Inorg. Chem.* **1987**, *26*, 4296–4298.
(51) Oertling, W. A.; Salehi, A.; Chung, Y. C.; Leroi, G. E.; Chang, C. K.; Babcock, G. T. *J. Phys. Chem.* **1987**, *91*, 5887–5898.
(52) Czernuszewicz, R. S.; Macor, K. A.; Li, X. Y.; Kincaid, J. R.; Spiro, T. G. *J. Am. Chem. Soc.* **1989**, *111*, 3860–3869.
(53) Kincaid, J. R.; Schneider, A. J.; Paeng, K. J. *J. Am. Chem. Soc.* **1989**, *111*, 735–737.
(54) Hashimoto, S.; Mizutani, Y.; Tatsuno, Y.; Kitagawa, T. *J. Am. Chem. Soc.* **1991**, *113*, 6542–6549.
(55) Han, S.; Ching, Y.-c.; Rousseau, D. L. *Proc. Natl. Acad. Sci. U.S.A.* **1990**, *87*, 8408–8412.
(56) Wikström, M. *Proc. Natl. Acad. Sci. U.S.A.* **1981**, *78*, 4051–4054.
(57) Yoshikawa, S.; Caughey, W. S. *J. Biol. Chem.* **1992**, *267*, 9757–9766.
(58) Wilson, E. B., Jr.; Decius, J. C.; Cross, P. C. In *Molecular Vibrations*; McGraw-Hill: New York, 1955; Chapter 4.

Table II. Calculated Frequencies for Vibrations of a Putative Fe—O—O—H Group and Parameters Used (cm^{-1} (PED%))[a]

	H_2O			D_2O		
	$^{16}O_2$	$^{16}O^{18}O$	$^{18}O_2$	$^{16}O_2$	$^{16}O^{18}O$	$^{18}O_2$
ν_{Fe-O}	787 (72)	782 (74), 753 (73)	749 (75)	798 (75)	796 (76), 767 (58)	764 (65)
ν_{OO}	561 (69)	548 (72), 547 (68)	535 (71)	526 (56)	518 (59), 516 (58)	507 (61)
δ_{OOH}	961 (95)	954 (94), 958 (96)	950 (96)	747 (64)	731 (67), 737 (44)	723 (54)
δ_{FeOO}	231 (99)	225 (94), 227 (96)	221 (95)	224 (95)	219 (94), 220 (96)	215 (95)
$\Delta\tau$	261 (99)	260 (100), 261 (99)	260 (99)	193 (99)	191 (99), 192 (100)	191 (99)
ν_{Fe-O} (obs.)	785	785, 751	751	796	796, 766	766

[a] Molecular structure parameters: torsion, τ_{OO} = 180° (trans form); valence angles, ∠FeOO = 120°, ∠OOH = 130°; bond lengths, Fe–O = 1.7 Å, O–O = 1.49 Å, O–H = 0.96 Å. Force constants (mdyn/Å for K and F; mdyn Å for H and P): K_{FeO} = 4.106, K_{OO} = 2.038, K_{OH} = 7.207, H_{FeOO} = 0.458, H_{OOH} = 0.421, P_{OO} = 0.020, F1 = 0.0083, F2 = 0.193.

and 796 and 767 cm^{-1} for Fe–O–O–D. Since they are sufficiently close to the values of the $^{16}O_2$ and $^{18}O_2$ derivatives, the ν_{Fe-O} RR bands for $^{16}O^{18}O$ might not be distinguishable from those of the $^{16}O_2$ and $^{18}O_2$ derivatives. On the other hand, the ν_{OO} frequency is calculated to be 561 cm^{-1} for $^{16}O_2$, 548 and 547 cm^{-1} for $^{16}O^{18}O$, and 535 cm^{-1} for $^{18}O_2$. Thus the expected behavior with $^{16}O^{18}O$ distinguishes between the ν_{Fe-O} and ν_{OO} modes. It is noted that the value of H_{OOH} used was smaller than that for H_2O_2,[49] and the value of K_{FeO} (4.1 mdyn/Å) is slightly larger than that for Fe–O_2 stretching (3.8 mdyn/Å), but considerably smaller than that for Fe^{IV}=O stretching (4.5 mdyn/Å). These features are indispensable to reproduce the upshift upon deuteration and may imply that the Fe–O bond in the Fe–O–O–H intermediate of CcO is slightly strengthened over the normal Fe^{III}–O single bond, while the O–O bond is appreciably weakened (K_{OO} = 2.0 mdyn/Å and ν_{OO} is calculated at 561 cm^{-1}) compared to that in H_2O_2 (K_{OO} = 3.8 mdyn/Å).[49]

The observed upshift of the 785-cm^{-1} band by 11 cm^{-1} upon deuteration is now satisfactorily reproduced in the calculated mode of ν_{Fe-O}. This upshift is due to vibrational coupling between the Fe–O stretching and the O–O–D bending modes, which becomes significant on account of the proximity of their frequencies but is insignificant for the Fe–O–O–H form. This coupling depends upon the torsion angle around the O–O bond; it was largest for 180° and smallest for 90° in the calculations mentioned above (not shown). We note that the present normal coordinate calculations provide a plausible interpretation of the observed isotropic frequency shifts by assuming structure I of Chart I but do not exclude a possibility of rather unexpected structure such as a protonated quasi-side-on structure like Fe–O(H)–O, for which structural as well as potential parameters are too ill-defined to perform normal coordinate calculations. More thorough theoretical treatments are desirable.

Assignment of the Band at 356 cm^{-1}. The nature of the band at 356 cm^{-1} is as follows: (1) It shows a downshift by 14 cm^{-1} upon $^{18}O_2$ substitution. (2) It shows little shift upon deuteration. (3) The band is distinctly narrower than those of other oxygen-isotope-sensitive bands (approximately half their width), suggesting homogeneity of the heme moiety. (4) The vibrational frequency depends primarily on only one of the oxygen atoms. A possible candidate within structure I is the Fe–O–O bending mode (δ_{FeOO}). This mode is calculated at 231 cm^{-1} for $^{16}O_2$, 227 and 225 cm^{-1} for $^{16}O^{18}O$, and 221 cm^{-1} for $^{18}O_2$, and since the two modes for $^{16}O^{18}O$ would not be resolved, eventually three bands are expected for the Fe–O–O–H form, contrary to the two bands observed (356 and 342 cm^{-1}). In fact, Proniewicz *et al.*[59] observed the RR spectrum of Fe^{II}(TPP) in an O_2 matrix at 30 K and found the δ_{FeOO} band at 349 cm^{-1} for $^{16}O_2$, at 347 cm^{-1} for $^{16}O^{18}O$, and at 345 cm^{-1} for $^{18}O_2$. Furthermore, this mode for Fe–O–O–H is expected to exhibit a downshift (7 cm^{-1}) upon deuteration, contrary to the observed absence of any shift. Thus, the assignment of the 356-cm^{-1} band to δ_{FeOO} is incompatible with the present observations. Furthermore, the 356/342-cm^{-1} bands are present in the spectrum of Figure 5C despite the absence of the 785/750-cm^{-1} bands. Therefore, it is unlikely that the 356/342-cm^{-1} bands can be ascribed to the hydroperoxy intermediate.

The other possible interpretation of the 356-cm^{-1} band is to assume the coexistence of other species with structures II or III of Chart I. If the 356-cm^{-1} band arises from a vibration of structure II or structure III, it implies either branching of the catalytic reaction[6] or else chemical equilibrium of two forms of an intermediate. Since there is no other positive evidence for this, one should be cautious about introducing structures II or III. Nevertheless, we think about their possibilities. All oxygen-isotope-sensitive vibrations of structures II and III are considered to be insensitive to deuteration and symmetric to the exchange of two oxygen atoms. For the side-on complex (structure III), whose ν_{OO} was identified around 800 cm^{-1},[46] the asymmetric Fe–O_2 stretching mode of Fe^{II}(TPP)O_2 was found at 408 cm^{-1} for $^{16}O_2$, shifting to 404 and 402 cm^{-1} for the $^{16}O^{18}O$ and $^{18}O_2$ derivatives, respectively.[59] The observed nature of the 356-cm^{-1} band of CcO is inconsistent with the properties expected for the side-on structure of the $^{16}O^{18}O$ adduct. It is desirable to determine the time course of the 356-cm^{-1} intensity precisely at different solution conditions and to compare it with those of the 804- and 785-cm^{-1} bands.

Character of the Ferryl Intermediate of CcO. In this study we assign the 804-cm^{-1} band to the ν_{Fe-O} mode of the ferryl intermediate. This band exhibits a downshift of 39 cm^{-1} upon $^{18}O_2$ substitution (Figure 4), which is in reasonable agreement with a theoretical value of 36 cm^{-1} expected for an isolated Fe=O harmonic oscillator with a frequency of 804 cm^{-1}. The ferryl hemes have been well characterized by RR spectroscopy for the second reaction intermediate (compound II) of horseradish peroxidase (HRP) and the corresponding intermediates of other peroxidases, as well as for porphyrin model compounds. Their Fe^{IV}=O stretching frequencies and the ^{18}O isotopic frequency shifts are summarized in Table III.

The ν_{Fe-O} frequency lies around 750–800 cm^{-1} for proteins in aqueous solution and around 820–850 cm^{-1} for model compounds in organic solvents. It is known that the ν_{Fe-O} frequency of HRP shows a pH-dependent change;[18,19] for HRP-C ν_{Fe-O} is observed at 775 cm^{-1} in neutral solution, but it is shifted to 788 cm^{-1} in alkaline solution, with the midpoint at pH 8.6. It is also known that ν_{Fe-O} is upshifted by 2–3 cm^{-1} in D_2O below pH 8.6 but not above this pH.[18,19] This observation was ascribed to the fact that the Fe^{IV}=O oxygen atom is hydrogen bonded in neutral but not in alkaline solution. Since the ν_{Fe-O} band of CcO does not show any peak in the H_2O/D_2O Raman difference spectrum (not shown), its Fe^{IV}=O oxygen must not be hydrogen bonded. Note that if we assume a structure like Fe^{III}—OH, the Fe—O stretching frequency should show a downshift upon deuteration, as is seen

(59) Proniewicz, L. M.; Paeng, I. R.; Nakamoto, K. *J. Am. Chem. Soc.* **1991**, *113*, 3294–3303.
(60) Palaniappan, V.; Terner, J. In *Biological Oxidation Systems*; Reddy, C. C., Hamilton, G. A., Madyastha, K. M., Eds.; Academic Press: San Diego, CA, 1990; Vol. 1, pp 487–503.
(61) Oertling, W. A.; Hoogland, H.; Babcock, G. T.; Weber, R. *Biochemistry* **1988**, *27*, 5395–5400.
(62) Hashimoto, S.; Teraoka, J.; Inubushi, T.; Yonetani, T.; Kitagawa, T. *J. Biol. Chem.* **1986**, *261*, 11110–11118.
(63) Reczek, C. M.; Sitter, A. J.; Terner, J. *J. Mol. Struct.* **1989**, *214*, 27–41.

Table III. Fe^{IV}=O Stretching Frequencies of Compound II of Peroxidases and Their Model Compounds[a]

species	$\nu_{Fe=O}$/cm^{-1}	$\Delta\nu(^{18}O)$/cm^{-1}	ref
CcO	804	39	present study
HRP-C (Compound II)	788 (alkaline)	34	18, 19
	774 (neutral)	34	18, 19
TP-1, 3 (Compound II)	788 (alkaline)		60
	771 (neutral)		60
MPO (Compound II)	782	35	61
CcP (Compound ES)	767	40	62
	753	28	63
LPO (Compound II)	745	33	63
(TPP)Fe^{IV}=O	852	34	64
(OEP)Fe^{IV}=O	852	35	64
(TMP)Fe^{IV}=O	843	33	65
(TpivPP)(THF)Fe^{IV}=O	829	37	66
(PPDME)(NMI)Fe^{IV}=O	820	36	67
(TPP)(NMI)Fe^{IV}=O	820	36	67
(OEP)(NMI)Fe^{IV}=O	820	35	67

[a] CcO, cytochrome *c* oxidase; HRP, horseradish peroxidase; TP, turnip peroxidase; MPO, myeloperoxidase; CcP, cytochrome *c* peroxidase; LPO, lactoperoxidase; TPP, tetraphenylporphyrin; OEP, octaethylporphyrin; TMP, tetramesitylporphyrin; TpivPP, picket fence porphyrin; THF, tetrahydrofuran; PPDME, protoporphyrin dimethylester; NMI, 1-methylimidazole.

for the Fe—O stretching band at 450 cm^{-1} for CcO.[25,26] It is also known for HRP that the oxygen atom is exchanged with that of bulk water in neutral but not in alkaline solution,[18] and the exchangeability seems to parallel the enzyme activity. In other words, when the Fe^{IV}=O oxygen is hydrogen bonded, oxygen exchange with bulk water takes place, and the Fe^{IV}=O complex is more rapidly converted to the ferric state.

As shown in Table III, (TPP)Fe^{IV}=O and (OEP)Fe^{IV}=O have their $\nu_{Fe=O}$ bands at the same frequency (852 cm^{-1}).[64] Presumably the nature of the Fe^{IV}=O bond is little affected by the type of porphyrin, although (OEP)Fe and (TPP)Fe yield different types of porphyrin π-cation radicals (a_{1u} and a_{2u}).[68] The Fe=O stretching frequency is sensitive to the trans ligand of oxygen, and indeed in (TPP)Fe^{IV}=O and (OEP)Fe^{IV}=O this frequency shifts down to 820 cm^{-1} when 1-MeIm is coordinated in the trans position.[67] The $\nu_{Fe=O}$ band of CcO was found at 804 cm^{-1}, similar to that of Mb,[69] while the corresponding bands of peroxidases are located in a lower frequency region (745–782 cm^{-1}).

One of the structural characteristics of peroxidases is the strong hydrogen bonding of proximal histidine and thus its imidazolate character.[70] This is reflected by the Fe–His stretching (ν_{Fe-His}) frequency, which is identified at 214 cm^{-1} for CcO,[71] at 220 cm^{-1} for Mb,[72] and at about 250 cm^{-1} for peroxidases.[70,73-75] Although the ν_{Fe-His} RR band has been observed only for the Fe^{II} high-spin state, there is a general trend that species with lower ν_{Fe-His} tend to give higher $\nu_{Fe=O}$.[76] It is believed that the anionic character of the proximal His stabilizes the higher oxidation state of the heme iron in the ferryl intermediate, and this may be related to the lower $\nu_{Fe=O}$. In this regard the Fe^{IV}=O heme of CcO is not particularly stabilized.

On the other hand, the reactivity of the Fe^{IV}=O oxygen is regulated by hydrogen bonding to it. Due to hydrogen bonding, the ferryl heme of the neutral HRP compound II is much more readily reducible than that of the alkaline one. This hydrogen bond is broken in alkaline solution, as evidenced by an upshift of $\nu_{Fe=O}$ by 14 cm^{-1}. The Fe=O stretching frequency of CcO is still higher than that of alkaline HRP compound II, suggesting that the Fe^{IV}=O oxygen of CcO is not hydrogen bonded, which would make the ferryl intermediate of CcO less reducible.

It is known that the terminal oxygen atom of the Fe^{II}–O–O group of MbO_2 is hydrogen bonded to distal His.[43] Due to the longer distance between the other oxygen atom and the distal His, there would be no hydrogen bond between the Fe^{IV}=O oxygen and the distal His in Mb, consistent with its higher $\nu_{Fe=O}$. These considerations lead us to suggest that the distal pocket of cytochrome a_3 is of the Mb type rather than of the HRP type, and the terminal oxygen of Fe^{II}–O–O of CcO is hydrogen bonded. This hydrogen bond becomes a covalent bond upon transfer of an electron to cytochrome a_3, and this process would be particularly accelerated upon raising the temperature from 5 to 30 °C. Since no hydrogen bond will be formed for the ferryl oxygen, the lifetime of the ferryl intermediate of CcO is relatively longer even at 30 °C.

Temperature Dependences of Reaction Intermediates and Enzymatic Reaction. As has been discussed, the bands at 571, 785, 804, and 450 cm^{-1} are considered to arise from the Fe^{II}—O_2, Fe^{III}—O—O—H, Fe^{IV}=O, and Fe^{III}—OH complexes, respectively, which are formed in this order. It has been reported that the oxidation of cytochrome *a* is concurrent with the decay of the Fe^{II}—O_2 complex, the extent of cytochrome *a* oxidation being as high as 60%.[55] Since the redox equilibrium between cytochrome *a* and Cu_A is sufficiently rapid,[77] it is more reasonable to deduce that the Fe^{II}–O_2 center of cytochrome a_3 receives an electron from the cytochrome *a*–Cu_A center rather than from Cu_B^I. Therefore, the formation of Fe^{III}–O–O–H is more likely than the formation of Fe^{III}–O–O–Cu^{II} when the electron-transfer pathway is taken into consideration. Although a competitive reaction involving electron transfer from Cu_B and thus the formation of Fe^{III}–O–O–Cu^{II} has been widely expected (but without any positive evidence), if the Cu_B^I ion were located very close to the bound O_2, the electron transfer from the Cu_B^I to the bound O_2 would be too fast to permit detection of any dioxygen adduct (Fe^{III}–O_2^-), the presence of which has, in fact, been observed. Therefore, the formation of Fe^{III}–O–O–Cu^{II}, if it takes place at all, must be accompanied by a fairly slow process of conformational change around Cu_B^I. On the other hand, the Fe^{III}–O–O–H porphyrin is extremely unstable under ordinary conditions, and we failed to detect its Raman band for an appropriate model compound at 77 K.[78] If the present band assignment is correct, the Fe^{III}—O—O—H intermediate of CcO is peculiar in that its Fe—O bond is moderately strong and its O—O bond is so weak. The Fe^{IV}=O heme of CcO has presumably no hydrogen bond, but it becomes Fe^{III}—OH upon receiving one more electron.

Figure 6 shows that the decay of the Fe^{II}–O_2 adduct is faster at higher temperatures, but the decay of the successive intermediate (Fe^{III}–O–O–H) seems to accelerate even more with

(64) Proniewicz, L. M.; Badjor, K.; Nakamoto, K. *J. Phys. Chem.* **1986**, *90*, 1760–1766.
(65) Mizutani, Y.; Hashimoto, S.; Tatsuno, Y.; Kitagawa, T. *J. Am. Chem. Soc.* **1990**, *112*, 6809–6814.
(66) Schappacher, M.; Chottard, G.; Weiss, R. *J. Chem. Soc., Chem. Commun.* **1986**, 93–94.
(67) Kean, R. T.; Oertling, W. A.; Babcock, G. T. *J. Am. Chem. Soc.* **1987**, *109*, 2185–2187.
(68) Czernuszewicz, R. S.; Macor, K. A.; Li, X. Y.; Kincaid, J. R.; Spiro, T. G. *J. Am. Chem. Soc.* **1989**, *111*, 3860–3869.
(69) Sitter, A. J.; Reczek, C. M.; Terner, J. *Biochim. Biophys. Acta* **1985**, *828*, 229–235.
(70) Teraoka, J.; Kitagawa, T. *J. Biol. Chem.* **1981**, *256*, 3969–3977.
(71) Ogura, T.; Hon'nami, K.; Oshima, T.; Yoshikawa, S.; Kitagawa, T. *J. Am. Chem. Soc.* **1983**, *105*, 7781–7783.
(72) Kitagawa, T.; Nagai, K.; Tsubaki, M. *FEBS Lett.* **1979**, *104*, 376–378.
(73) Teraoka, J.; Job, D.; Morita, Y.; Kitagawa, T. *Biochim. Biophys. Acta* **1983**, *747*, 10–15.
(74) Babcock, G. T.; Ingle, R. T.; Oertling, W. A.; Davis, J. C.; Averill, B. A.; Hulse, C. L.; Stufkens, D. J.; Bolscher, B. G. J. M.; Wever, R. *Biochim. Biophys. Acta* **1985**, *828*, 58–66.
(75) Kitagawa, T.; Hashimoto, S.; Teraoka, J.; Nakamura, S.; Yajima, H.; Hosoya, T. *Biochemistry* **1983**, *22*, 2792–2796.
(76) Oertling, W. A.; Kean, R. T.; Wever, R.; Babcock, G. T. *Inorg. Chem.* **1990**, *29*, 2633–2645.
(77) Morgan, J. E.; Li, P. M.; Jan, D.-J.; El-Sayed, M. A.; Chan, S. I. *Biochemistry* **1989**, *28*, 6975–6983.
(78) Tajima, K. *Inorg. Chim. Acta* **1989**, *163*, 115–122.

increasing temperature, since the reduction in intensity of the 785-cm^{-1} band upon raising the temperature is more marked than that of the 571-cm^{-1} band. In contrast, the intensity of the 804-cm^{-1} band increases at higher temperatures. This means that the reduction of the Fe^{IV}=O complex is less temperature dependent than the reduction of Fe^{III}–O–O–H.

The exchange of the OH^- group of CcO with that of bulk water seems to be noticeably accelerated at higher temperatures, because the Fe^{III}–OH stretching $^{16}O_2/^{18}O_2$ difference peak becomes very weak at 30 °C. It would be interesting to compare the present results with those of kinetic absorption experiments using the flow-flash technique of Oliveberg *et al.*[8]

Varotsis and Babcock[24] initially reported the insensitivity of their 790-cm^{-1} band to deuteration, but very recently they reinvestigated this band with $^{18}O^{16}O$,[79] correcting their results to be deuteration sensitive, in consonance with two other observations.[25,26] However, the present study can interpret Varotsis and Babcock's first results reasonably in terms of the temperature effects. If the effective temperature of their sample in their first experiment was close to 30 °C, the main intermediate present at $\Delta t = \sim 1$ ms would be the Fe^{IV}=O intermediate, which should give rise to the deuteration-insensitive 804-cm^{-1} band. When the effective temperature of the sample is lowered, the contribution from the Fe–O–O–H intermediate to the unresolved 800-cm^{-1} band increases, and it becomes dominant at 5 °C for the same delay time. Therefore, the unresolved 800-cm^{-1} band would exhibit an upshift upon deuteration. Their recent results[79] are rather puzzling in the sense that the deuteration-sensitive 790-cm^{-1} band is coexistent with the 458-cm^{-1} band assigned to the Fe^{III}–OH species.

In conclusion, we established that the Fe_{a3}^{II}–O_2 complex (compound A) obtained previously is of an end-on type on the basis of the observed data for the $^{16}O^{18}O$ derivatives and simulation calculations and that the Fe_{a3}^{III}–O–O–H species with a marker band at 785 cm^{-1} is generated as an intermediate following the dioxy complex and is subsequently converted to the Fe^{IV}=O species, by using the high-resolution time-resolved RR technique and the $^{16}O^{18}O$ derivatives. We have reassigned the oxygen-isotope-sensitive RR bands.

Acknowledgment. We are grateful to Dr. Y. Mizutani for help with the normal coordinate calculations. This study was supported by Grants-in-Aid of the Ministry of Education, Science, and Culture, Japan, for Priority Areas (Bioinorganic Chemistry) to T.K. (04225106) and (Cell Energetics) to T.O. (04266105) and for Encouragement of Young Scientists to T.O. (04780281). The preparation of $^{16}O^{18}O$ at Argonne National Laboratory was carried out under the auspices of the Office of Basic Energy Sciences, Division of Chemical Sciences, U.S. Department of Energy, under Contract W-31-109-Eng-38.

(79) Varotsis, C.; Zhang, Y.; Appelman, E. H.; Babcock, G. T. *Proc. Natl. Acad. Sci. U.S.A.* **1993**, *90*, 237–241.